JOURNAL OF MATERIALS SCIENCE **40** (2005) 3639–3650

A new understanding of near-threshold damage for 200 keV irradiation in silicon

N. STODDARD*
Materials Science and Engineering Department, North Carolina State University, Raleigh, NC, 27695-7916, USA
E-mail: ngstodda@ncsu.edu

G. DUSCHER
Materials Science and Engineering Department, North Carolina State University, Raleigh, NC, 27695-7916, USA; Condensed Matter Science Division, Oak Ridge National Laboratory, Oak Ridge, TN 37831, USA

W. WINDL
Materials Science and Engineering Department, The Ohio State University, Columbus, OH 43210-1178, USA

G. ROZGONYI
Materials Science and Engineering Department, North Carolina State University, Raleigh, NC, 27695-7916, USA

Recently we reported room temperature point defect creation and subsequent extended defect nucleation in nitrogen-doped silicon during 200 kV electron irradiation, while identical irradiation of nitrogen-free silicon produced no effect. In this paper, first principles calculations are combined with new transmission electron microscope (TEM) observations to support a new model for elastic electron-silicon interactions in the TEM, which encompasses both nitrogen doped and nitrogen free silicon. Specifically, the nudged elastic band method was used to study the energetics along the diffusion path during an electron collision event in the vicinity of a nitrogen pair. It was found that the 0 K estimate for the energy barrier of a knock-on event is lowered from ~12 to 6.2 eV. However, this is still inadequate to explain the observations. We therefore propose an increase in the energy barrier for Frenkel pair recombination associated with N_2-V bonding. Concerning pure silicon, stacking fault formation near irradiation-induced holes demonstrates the participation of bulk processes. In low oxygen float zone material, 2–5 nm voids were formed, while oxygen precipitation in Czochralski Si has been verified by electron energy-loss spectroscopy. Models of irradiation-induced point defect aggregation are presented and it is concluded that these must be bulk and not surface mediated phenomena.

1. Introduction

The use of nitrogen doping in high purity silicon has been a topic of much research in recent years [1]. Both Czochralski (CZ) and Float Zone (FZ) single crystal silicon wafers benefit from the introduction of low concentrations ($<10^{15}$ cm^{-3}) of nitrogen. Specifically, nitrogen-doped Czochralski silicon (N-CZ Si) has increased denuded zone integrity and size [2], along with a higher density of smaller oxygen precipitates in the bulk which provides improved gettering ability compared to nitrogen free CZ Si [3]. Although the oxygen precipitate growth rate and size are limited by oxygen diffusion, which requires high temperatures, the precipitate density is independent of annealing temperature since they grow from nuclei that exist in the as-grown N-CZ Si [3]. Theoretical work [4] suggests that the split-interstitial N_2 complex is quite stable and tends to form vacancy complexes, either as VN_2 or, more prevalently, V_2N_2. These complexes tie up vacancies at high temperature and reduce the formation of voids by delaying their onset through lowering their formation temperature during cooling [5].

Evidence of Frenkel pair defect generation and interaction with impurities under a 200 kV transmission electron microscope (TEM) beam have recently been observed in CZ Si that has a bulk nitrogen doping of 10^{15} cm^{-3}, whereas there was no effect in nitrogen-free silicon [6].During irradiation, the Frenkel pairs

*Author to whom all correspondence should be addressed.

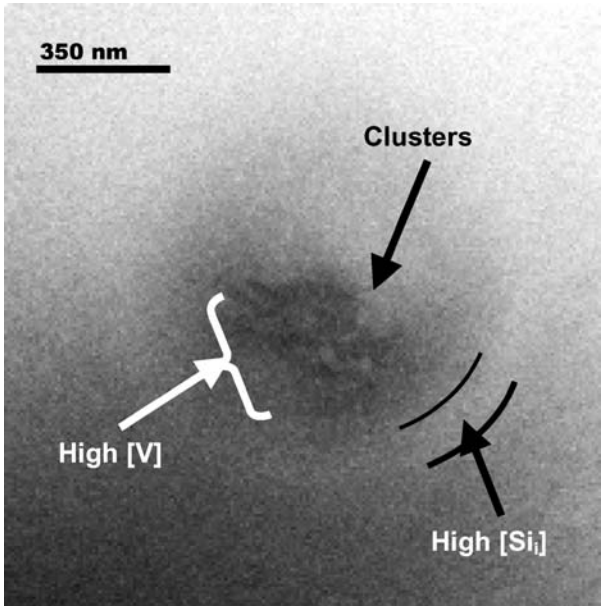

Figure 1 STEM Z-contrast image of N-CZ Si irradiated area. A central dark area is attributed to a large concentration of vacancies while the brighter ring surrounding it is attributed to excess self-interstitials. Some modulation of contrast exists in the dark region, suggesting clustering.

created by knock-on electron collisions do not all recombine, due to the presence of nitrogen and its complexes. Instead, the nitrogen can form complexes with the newly formed vacancies, permanently separating the interstitial silicon of the Frenkel pair from its vacancy. The interstitial atoms, stimulated by further electron collisions, diffuse away from the e-beam irradiated zone, leaving behind nitrogen related complexes that either accumulate vacancies to produce voids, or complex with oxygen atoms to facilitate SiO_2 nucleation. The benefit of this nanoscale TEM laboratory is that normally high-temperature extended defect nucleation processes are observed at room temperature in an area of the TEM operator's choosing.

An example from this laboratory is shown in Fig. 1, a Z contrast scanning TEM (STEM) image of an N-CZ Si sample, previously presented in Ref. [6]. An irradiation was performed for 45 minutes in the center of the area with a beam diameter of ∼400 nm. In Z-Contrast images, the signal is derived from electrons scattered via Rutherford back scattering (RBS) to a high angle and measured by an annular detector. Since elements with higher Z have stronger RBS, they provide a stronger signal, as do denser and thicker areas of the same elemental composition [7]. In Fig. 1, the material is high purity silicon, so elemental contrast is ruled out. A thickness gradient, due to the wedge shape of the TEM sample, can be seen going from the lower left to the upper right of the micrograph. Atomic force microscope measurements have verified that the topography of the irradiated area is flat, so the circular features observed must be due to density differences. In Fig. 1, the center of the image appears dark while a bright ring can be discerned just outside of the irradiated area. Since we have already ruled out Z and thickness variations, the beam-induced dark/bright contrast are attributed to local density variations. Specifically, the center of the image is vacancy enriched, while the bright ring has an excess of interstitials. The Frenkel pair generation process described above has occurred during the irradiation, and the self-interstitials have at least partially diffused outside of the irradiated region, stimulated by collisions with beam electrons as well as thermal energy. The difference in behavior between vacancies and interstitials bares a moment's discussion. While vacancies and interstitials in silicon have similar migration energies (∼0.3 eV) [8], the situation is different when electron stimulation is added to the equation. When an interstitial atom is given kinetic energy in a collision, it can take multiple jumps as a result. When an atom adjacent to a vacancy is stimulated, it can still make only one jump. Thus, while both species have been observed to diffuse at room temperature [9], we expect interstitials to diffuse faster than vacancies during electron irradiation, partially accounting for the spatial separation. Another consideration is the interaction of the nitrogen, which complexes readily with vacancies to form the very stable and immobile N_2V complex [4]. This factor will be investigated extensively later on. In CZ Si, the central vacancy-rich environment should be favorable for oxide formation because of the generous free volume available for the precipitation related expansion, as well as the supersaturation of oxygen. In fact, small clusters are observed near the center of Fig. 1, and closer inspection provided evidence of secondary phase formation, although the chemical composition was not determined [6]. Similar experiments on nitrogen-free CZ and FZ silicon reference samples under identical TEM preparation and irradiation conditions yielded no damage, suggesting that separation of the Frenkel pair components and subsequent interactions depend on the bulk nitrogen concentration or nitrogen-related complexes. In this paper, similar clusters and aggregates will be identified using electron energy-loss spectroscopy (EELS), and the nucleation process will be discussed. In addition, nitrogen-doped float zone samples have been irradiated and analyzed. The interesting factor in FZ samples is the reduced oxygen concentration (a factor of 1000 less than CZ Si), which has important consequences for mechanical and electrical properties of wafers, in addition to precipitation behavior.

2. Theory of electron-silicon interactions

The electrons of the TEM beam carry 200 keV of energy, giving them relativistic speeds with $v/c = 0.695$. Interactions with atoms in a crystalline solid can be either elastic or inelastic. Inelastic scattering gives rise to a diffuse background of electrons that have lost relatively little energy from interactions with valence electrons, core electrons, phonons, etc. Elastic (or energy-conserving) scattering of electrons from the screened nucleus gives rise to diffraction patterns, so-called HOLZ lines and, at higher scattering angles, a small background of Rutherford back-scattered electrons. It is the electrons scattered to large angles that are of greatest interest here, since they can transfer their entire momentum to the target atom. Momentum conservation limits the amount of energy that can be transferred, and in the case of a silicon atom, the energy transferred, T,

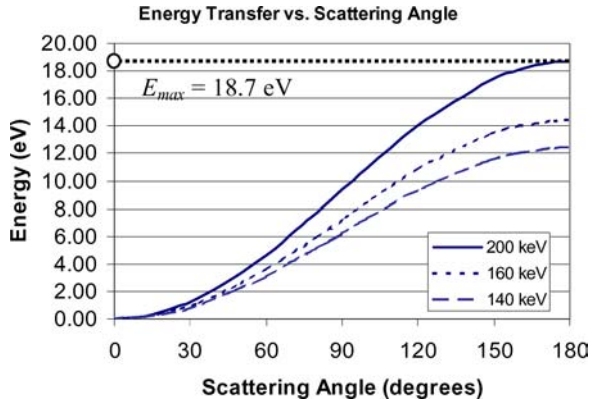

Figure 2 Energy imparted to silicon as a function of recoil angle for electrons of 140 kV, 160 kV and 200 kV.

by an electron scattered to an angle θ is

$$T = \frac{2E_e}{m_{\mathrm{Si}}c^2}(E_e + 2m_e c^2)\sin^2\frac{\theta}{2}$$

where E_e is the electron energy, c is the speed of light and m_e is the electron rest mass. The maximum possible transferred energy, corresponding to $\theta = 180$, is $T_{\max} = 18.7$ eV [10]. The full plot of transferred energy vs. scattering angle is given in Fig. 2 for electrons of 140, 160 and 200 keV. The number of Frenkel pairs, N_{FP}, created from a knock-on collision is described by the modified Kinchin-Pease expression

$$N_{\mathrm{FP}} = \begin{cases} 0 & T < E_d \\ 1 & E_d \le T \le 2.5E_d \\ 0.4E_D/E_d & 2.5E_d < T \end{cases}$$

where T is the imparted energy and E_d is the displacement energy for the material. For silicon, experiments suggest that E_d ranges from 12–20 eV while theoretical studies have indicated that it might be as low as 10 eV, and depends on the crystallographic orientation [10, 11], For the lowest theoretical values, there have been suggestions that Monte Carlo simulations for longer periods of time result in recombination of the Frenkel pair, so that the spontaneous recombination volume (SRV) is larger at 300 K than *ab initio* calculations might predict. If the effective displacement energy is less than 18.6 eV for a given zone-axis alignment, then one would expect Frenkel pairs to be created during 200 kV electron irradiation. Under normal operating conditions, with a beam diameter greater than 10 nm, damage accumulation is not observed. Even though it is commonly quoted that the minimum TEM beam energy to create Frenkel pairs in Si is 140–160 keV, which corresponds to a maximum energy transfer of 12.4–14.4 eV to silicon, damage is typically only seen under conditions where the beam is converged to a diameter of ~5 nm, at which point a hole can develop in the thin foil. Another notable exception to the absence of radiation damage is the use of sample cooling. In an experiment by Yamasaki and Takeda where the sample temperature was maintained at 15 K, some permanent damage formation became evident after exposure to a dose of $3 \times 10^{23}/\mathrm{cm}^2$ [12]. This affirms the earlier conjecture about temperature effects on the SRV, and suggests that Frenkel pairs are created during the course of 200 kV irradiation under all irradiation conditions; at normal temperatures (300–400 K), the Frenkel pairs recombine soon after the collision, but at low temperatures the damage is frozen in. A second important conclusion in Yamasaki's study, agreeing with that of Seidman *et al*. [13], is that amorphization of silicon is extremely difficult below 1 MeV of accelerating energy, even at low temperature. Yamasaki and Takeda conclude from this that the introduction of one-at-a-time Frenkel pairs is insufficient for amorphization, but that damage cascades are the nuclei for amorphization. This will be revisited based on the results presented below.

To determine the probability of a knock-on collision, one starts with the scattering cross section. The differential Mott cross section for elastic scattering provides a relativistic correction to the Rutherford expression as follows [14]

$$\left(\frac{d\sigma}{d\Omega}\right)_{\mathrm{Rutherford}} = \left(\frac{Ze^2}{8\pi\varepsilon_0 E}\right)^2\left(\frac{E+E_0}{E+2E_0}\right)^2\frac{1}{\sin^4\frac{\theta}{2}}$$

$$\left(\frac{d\sigma}{d\Omega}\right)_{\mathrm{Mott}} = \left(\frac{d\sigma}{d\Omega}\right)_{\mathrm{Rutherford}} \times \left\{1 - \beta^2\sin^2\frac{\theta}{2} + \pi\alpha\beta\sin\frac{\theta}{2}\left(1 - \sin\frac{\theta}{2}\right)\right\}$$

where Z is atomic number, E is the electron energy, E_0 is the electron rest energy, e is the electron charge, ε_0 is the vacuum permittivity, θ is the scattering angle, $\alpha = Z/137$ and $\beta = v/\mathrm{c}$. The cross-section for imparting *at least* a given value of energy $T(\theta)$ (i.e. scattering to greater than a given scattering angle $\theta_{\min}$) can be derived from the differential cross-section by integration.

$$\sigma_{\mathrm{Mott}}(T) = \int_{\theta_{\min}}^{\pi}\left(\frac{d\sigma}{d\Omega}\right)_{\mathrm{Mott}} 2\pi\sin(\theta)d\theta$$

To translate the cross section into a probability, one can first convert the cross section into an angle-dependent mean free path [15].

$$\lambda_{\mathrm{elastic}}(\theta) = \frac{1}{\sigma_{\mathrm{Mott}}n_a}$$

where n_a is the number of atoms per unit volume. The probability is then defined by Poisson statistics in terms of the ratio of the sample thickness, t, to the mean free path, λ.

$$P_{\mathrm{elastic}}(t,\theta) = \frac{t}{\lambda_{el}}e^{-t/\lambda_{el}}$$

The probability for a collision that transfers energy greater or equal to a given value is plotted in Fig. 3, so that the probability of a knock-on event can be determined.

3. Materials and methods

[100] oriented, as-grown N-FZ and N-CZ plan-view samples were prepared by conventional TEM thinning methods, which include grinding, polishing, dimple grinding and ion milling. Siltronic Corp. grew the N-CZ starting material while the N-FZ sample came from the National Renewable Energy Labs. The N-CZ sample has bulk light element impurity profiles of [O] $= 7 \times 10^{17}$ cm^{-3} and [N] $= 10^{15}$ cm^{-3} while the N-FZ sample has [O] $= 10^{15}$ cm^{-3} and [N] $= 10^{15}$ cm^{-3}. Samples from these wafers were prepared for TEM analysis by mechanical polishing, dimple grinding and ion milling with 3–5 keV Ar^+ ions at 5–6 mA. It has been shown elsewhere that this type of sample preparation can result in enhanced bulk nitrogen concentrations of up to 10^{16} cm^{-3} [16]. Separately, a piece of the sample from the as-grown N-CZ Si was annealed using a hi-lo cycle of 16 h at 1050°C and 8 h at 750°C. It was prepared as a cross-sectional TEM sample and [110] oriented for irradiation. All electron irradiation was performed at 200 kV in JEOL 2010F and Topcon 002B electron microscopes, while high-resolution imaging, EELS, and scanning TEM (STEM) in Z-Contrast and bright field modes were performed on the JEOL instrument. It should be noted that contamination issues during the irradiation are minimized because the samples undergo plasma cleaning every time they are placed in the microscope, and Z-contrast analysis is typically done at a different time than the irradiation.

Simulations were performed using the Vienna *Ab Initio* Simulations Package (VASP), which employs a self-consistent approach based on density functional theory in the local density approximation. Ultra-soft pseudopotentials with a plane-wave basis set were used both for ionic relaxation and for calculating the total energy at different points along the diffusion path. A perfect supercell of 64 silicon and two nitrogen atoms, i.e. eight unit cells, was first relaxed with the well-known N_2 structure consisting of two nitrogen and two silicon atoms in a square configuration in the [110] direction. A similar configuration with the nearest silicon atom to the N_2 pair situated in a near-by interstitial position was relaxed, and four to six intermediate positions between these two were interpolated as starting guesses for nudged elastic band calculations. Each of the intermediate steps was then locally relaxed along its hypertangent to a total energy tolerance of 0.005 eV. Only the neutrally charged case is considered, since in other work the energy difference between negative and neutral charge states was negligible while the positive charge state had higher energies by a constant energy shift [17].

4. Results

4.1. Czochralski silicon

Fig. 4 depicts an irradiated N-CZ Si sample in both bright field and Z-Contrast modes of the STEM. The dark and light arcs visible in 4(a) and 4(b), respectively, delineate the boundary of the irradiated region. The irradiation was positioned near the edge of the TEM foil for best results in Z-Contrast and EELS modes of the

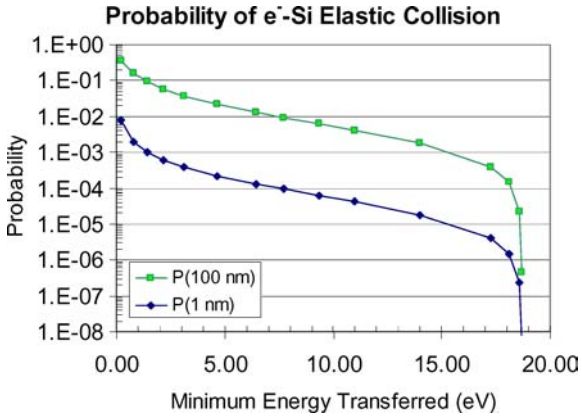

Figure 3 Probability for energy transfer by a 200 kV electron to a silicon atom as a function of transferred energy.

TEM. In Z-Contrast images 4(b), 4(c) and 4(d), the low signal dark areas correspond to a high concentration of vacancies, while the high signal bright areas are denser (i.e. interstitial rich) or thicker, as was the case in Fig. 1. As noted earlier, Z-Contrast image features are generally due to differing elemental distributions (based on atomic number Z), varying sample thickness or density fluctuations [7]. Since this sample is pure CZ silicon (the nitrogen influence is negligible), we can attribute the contrast to local Si density variations due either to vacancies or silicon self-interstitials, local thickness differences or the presence of extra layers of oxide. It should be noted that silicon dioxide is very close in mass density to normal silicon, but since RBS goes as Z^2, an oxide layer will give less signal than an equal thickness of silicon. If, on the other hand, extra oxide thickness is on top of an equal thickness of silicon, the signal will be additive and give higher contrast to this region. Previously, secondary phases were observed but not identified. Here, as in Figs 4c and d, EELS chemical analysis shows that high oxygen concentrations exist both inside the large irradiated region and in a speckled ring just outside of it. Elastic collisions resulting from TEM electron bombardment will enhance oxygen diffusion in the same manner as for silicon interstitials. For oxygen diffusing in a vacancy-rich environment, the eventual result will be clustering and precipitation. Ripening of oxygen clusters inside the irradiated zone has been observed as longer irradiation times are used, a process that competes with diffusion out of the beam volume. While nitrogen concentrations were too small for measurement by EELS, the oxygen is readily detected and has some dramatic effects. Consider, for example, the two large bright spots in Figs 4c and d. The sharply defined EELS spectra, see Fig. 4e, for the boxed area in Fig. 4c clearly indicates the presence of pure silicon dioxide, based on the sharp peak at 106 eV. Within the Si L-edge profile, the first sharp peak corresponds to stoichiometric silicon dioxide while the second peak relates to the strong presence of interstitial oxygen. The Fig. 4c particle has fairly distinct boundaries, while the bright area in 4d has softer edges and is a mix of silicon with interstitial oxygen and silicon dioxide, as indicated by its EELS spectrum. No particle like either of these two was found elsewhere

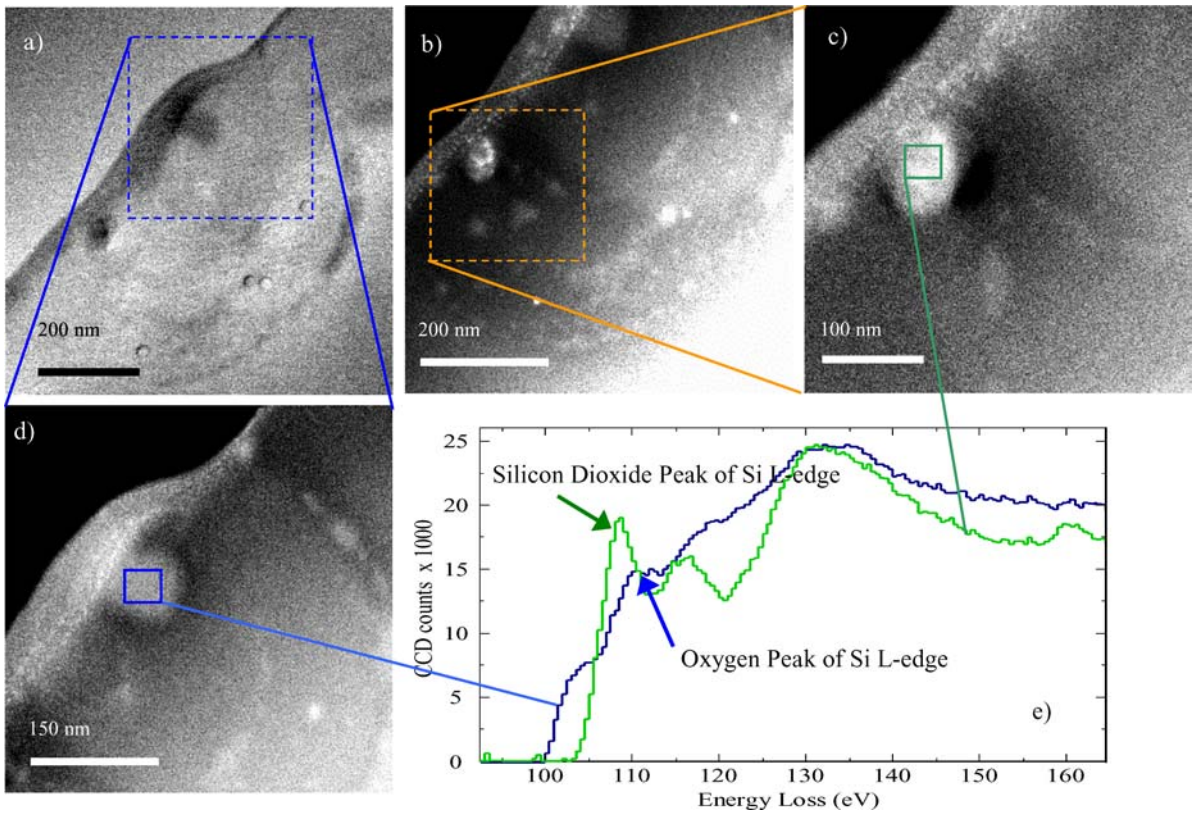

Figure 4 200 kV Scanning TEM images of an e-irradiated region of a N-Cz Si sample. (a) is a bright field image while (b), (c), and (d) are Z-Contrast images revealing bright clusters inside and peripheral rings surrounding the irradiated area. (e) is an electron energy loss spectrum from two of the particles nucleated during irradiation. The particle in (c) is identified as stoichoimetric silicon dioxide by the peak at 106 eV in the Si $L_{2,3}$ edge. The particle in (d) is mostly composed of silicon with interstitial oxygen.

in the sample, i.e. outside of the irradiated zone, and they were not present before irradiation. As such, they must be attributed to e-beam-induced clustering and precipitation.

4.2. Float zone silicon

In nitrogen-doped, low oxygen float zone silicon, the same separation of interstitials and vacancies occurs as was described above for N-CZ samples, see Fig. 5. From this observation, it can be concluded that interstitial oxygen is not the key factor in e-beam induced Frenkel pair separation. With a lower interstitial oxygen concentration, no bright clusters appear in the center of the irradiated region, and high-resolution imaging provided no evidence of second phase formation. The irradiated area appears in Fig. 5b as a dark circle whose weaker contrast corresponds to a lower concentration of silicon atoms, i.e. a higher concentration of vacancies. The differences in the response to irradiation extend beyond the lack of oxygen precipitates. Instead of the aggregation of oxygen, we observed void formation due to the agglomeration of vacancies during irradiation. Evidence of this phenomenon can be found in Fig. 5. First, it should be noted that the three bright spots in Fig. 5b are due to carbon contamination while the converged Z contrast e-beam rested in spot-mode at those positions. Even though carbon has a lower Z than silicon, these spots appear bright because of the thickness of the carbon added on top of the sample thickness. Closer examination of the irradiated area in Z contrast mode reveals small dark features, see Fig. 5c. By the same logic as is used above, these can only be aggregates of vacancies. Their triangular appearance when viewed in high resolution suggests that the voids are somewhat faceted and vary in size from 2–5 nm, see Fig. 5d. In this case, the vacancies have had sufficient time to aggregate into voids without the interference of oxygen. A diffuse brighter halo of excess interstitials surrounds the dark circle, as was the case for N-CZ Si. In addition to the halo, faint bright lines can be seen directed radially away from the ring, and corresponding to the open (110) directions. The implication of this result is that the interstitial diffusion can continue outside of the irradiated region in certain directions. This is not necessarily surprising since the sample is maintained in the TEM at a temperature below 350 K, while diffusion of silicon self-interstitials has been reported below 100 K [9]. It is also a reinforcement of the bulk nature of the diffusion, since channeling along (110) directions is a significantly weaker phenomenon in surface diffusion.

The results of different intensities of irradiation are found in Fig. 6. In 6a, a hole has been created by intense convergent beam irradiation of the N-CZ Si thin foil. This type of hole formation by electron irradiation has been widely observed in thin film silicon samples, and is generally attributed to surface diffusion [18]. The interesting result here is that a stacking fault has nucleated in close proximity to the hole, presumably formed from

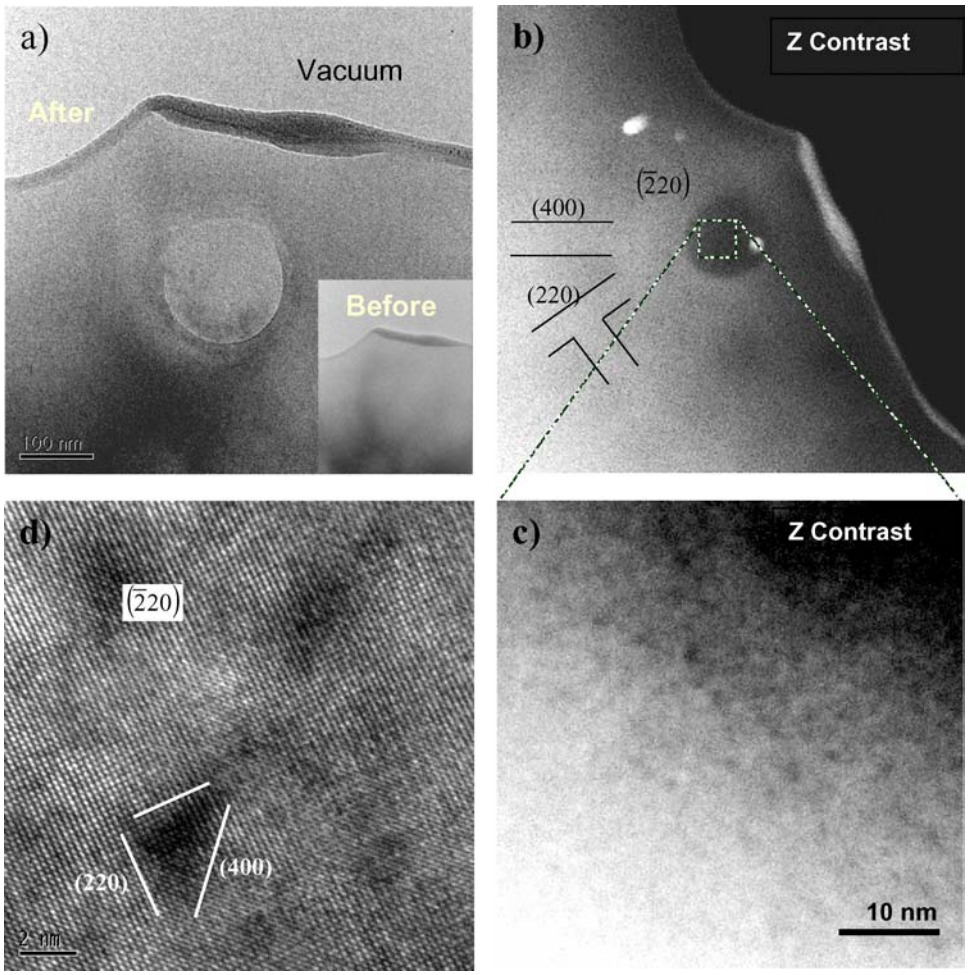

Figure 5 TEM images of a N-FZ Si sample after irradiation. (a) is a conventional TEM image of N-FZ Si irradiated for 10 min in a JEOL 2010F TEM. (b) is the same region imaged in Z Contrast STEM mode: no bright speckles exist in the dark vacancy-rich region, but faint bright lines emanate from the center along crystallographic directions. (c) is a higher magnification image of the vacancy-rich dark circle, revealing small voids, imaged as faceted dark pits. (d) is a high-resolution conventional image of the area in (c).

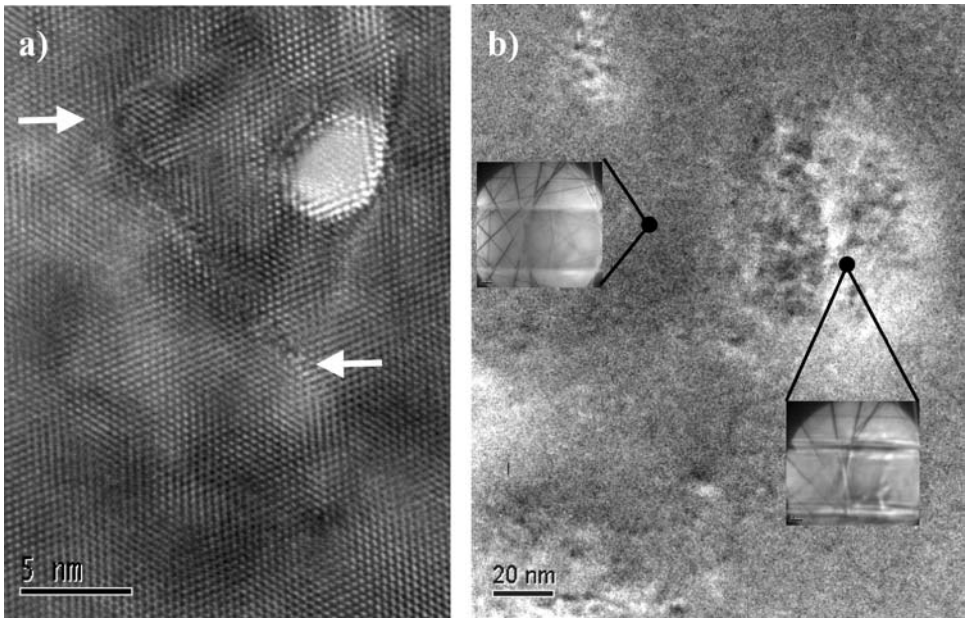

Figure 6 Tightly Converged Beam Irradiation: (a) The interstitials ejected from the 3 nm irradiation area during hole formation diffuse into the bulk and coalesce to form a stacking fault, whose ends are indicated by white arrows. (b) With a larger 60 nm beam, amorphization of the silicon substrate occurs.

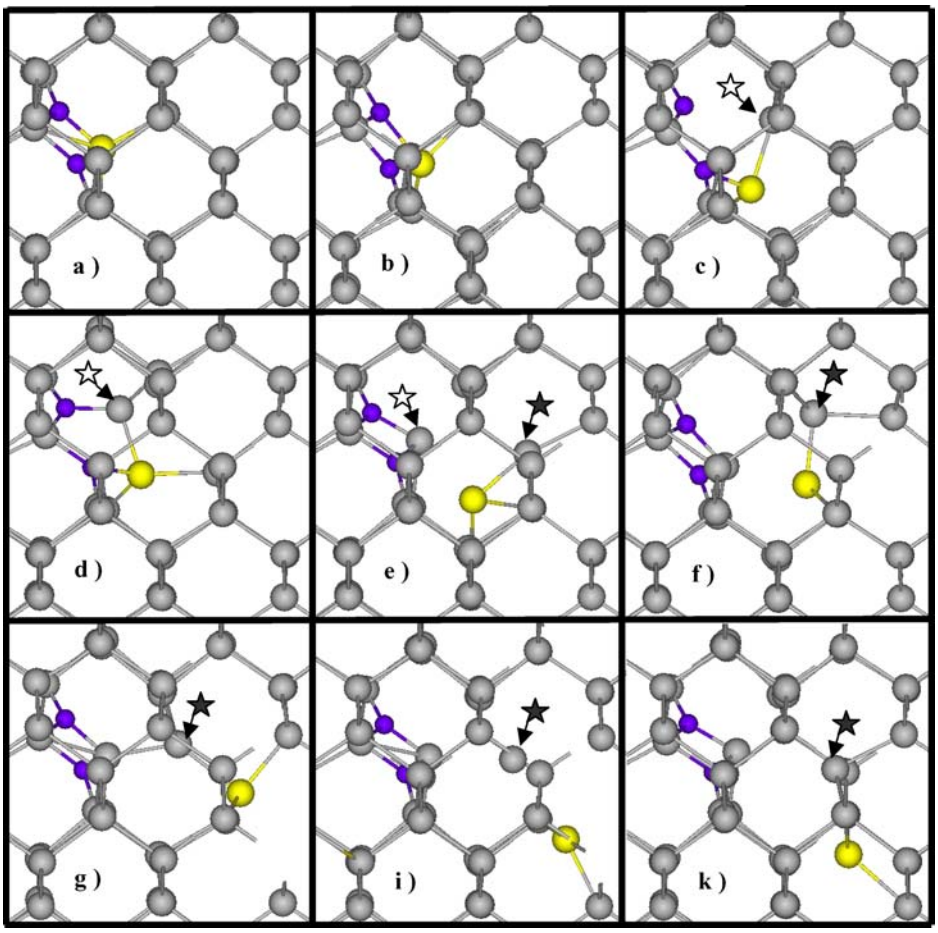

Figure 7 [110] projection of the diffusion path determined by *ab initio* nudged elastic band calculations for an excited silicon atom (in yellow) knocked away from an N_2 pair (in purple) and into a nearby interstitial position. The stable N_2 square configuration of 7(a) re-forms with a new atom by 7(e), resulting in an N_2V complex near a self-interstitial, 7(k).

atoms diffusing in the bulk by interstitial paths away from the beam. With a beam of ~60 nm diameter, as in Fig. 6b, amorphization of the silicon crystal occurs but a hole is never formed. The amorphous nature of the irradiated region is verified by convergent beam electron diffraction patterns (inset), where the crystalline diffraction contrast is mostly lost in the irradiated area.

4.3. Theoretical results

The electron knock-on process observed in nitrogen-doped silicon was studied using a nudged elastic band calculation to determine how the nitrogen enables Frenkel pair separation. First, one of the silicon atoms nearest the nitrogen pair was moved along the [110] direction to the nearest stable interstitial position. Nine positions in between the two configurations were progressively interpolated to determine the lowest energy diffusion path for the excited silicon atom. The configurations along the path of the knock-on event are shown in Fig. 7, while the energetics can be found in Fig. 8. The initial configuration is the well-known and very stable N_2 configuration, see Fig. 7a; one of its nearest neighbors is then displaced on a path towards the final configuration on a nearby tetrahedral interstitial site, see Fig. 7k. There are two saddle points along this path: at 4.2 eV above the ground state in Fig. 7e and at 6.2 eV above the ground state, found in Fig. 7j. Two

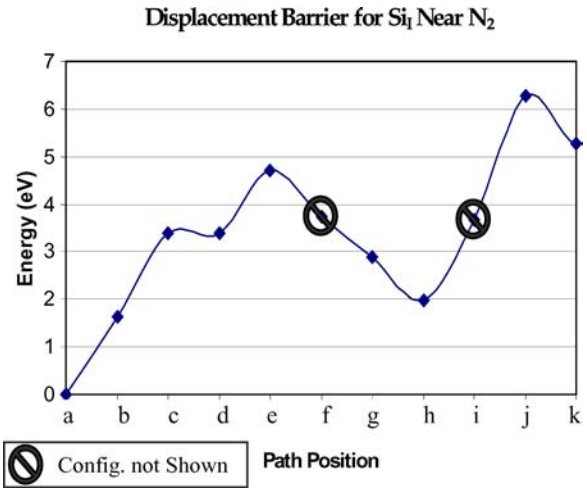

Figure 8 Energy profile of the diffusion path shown in Fig. 7. An initial 4.7 eV migration barrier leads to a local minimum at 2.0 eV above the ground state that will revert to the ground state if the excited atom does not have the 6.2 eV necessary to escape to the next nearest interstitial position. Black and white stars follow two atoms of interest.

of the configurations, (f) and (i) in Fig. 8, are omitted because they provide no interesting information. The excited atom, highlighted in yellow, moves away from the N_2 pair. Meanwhile, a nearby atom is drawn in to re-form a [110]-oriented N_2 square, see the white star in Figs 7c–e. Configuration 7e is a local saddle point, proceeding to a local minimum in 7h. In the series from

7e–k, the atom indicated by the black star is kicked out to accommodate the excited atom, and in Fig. 7h, the system is very close to reverting to the original configuration with three atoms exchanged. If the excited atom (highlighted) does not have the energy to move through the saddle point of Fig. 7j, there would be no observable change and no net damage. In the case that the excited atom moves to the final configuration, the atom indicated by the black star determines where the vacancy ends up; the lower energy configuration, shown in 7k is for a VN_2 complex to form. This is the first configuration that is stable against reversion to something equivalent to Fig. 7a, with a 1 eV energy drop from 7j to 7k. The total formation energy for the final configuration is 5.3 eV. To evolve the system one step beyond 7k, a similar calculation was carried out to find the energy barrier between this interstitial position and the next interstitial position, one step farther from the N_2 pair. To get the excited atom farther away, a supercell of twice the size, 128 atoms, was used with 64 atoms of pure Si added. The energies of the initial and final interstitial states are within 0.2 eV, with an intermediate saddle point at 1 eV higher energy than 7k. This value for the migration barrier energy is still higher than for bulk diffusion, indicating some residual pull on the interstitial atom.

5. Discussion

5.1. Surface considerations

The surface is a consideration that must be taken into every interaction in a thin foil. In this case, it might be tempting to explain the effects noted in Figs 1, 4 and 5 as surface related. The argument would be that only the atoms on the surface are being manipulated to move outside of the beam, and that the resulting thickness variation causes the ring-shaped contrast. In the case of the oxide formation in Fig. 4, one might surmise that the silicon dioxide particles have simply coalesced from the native surface oxide. For Fig. 5, the dark spots could be faceted [111] surface pits, once again the result of surface manipulation. There are several problems with these arguments, however. First of all, there is the response of the nitrogen-free reference samples, which exhibit essentially no response to irradiation with beams larger than 10 nm in diameter. In some N-free samples, slight stress contours were discernible after irradiation, but in most even this was lacking, and in no N-free sample were there features like those in the Z- contrast micrographs. In the study by Yamasaki and Takeda [12], damage could only be created in Si under 200 kV irradiation by cooling the sample down to 15 K. The only difference between the N-free reference samples (similar to those used in [12]) and the N-doped samples was the bulk nitrogen concentration, so that the fundamental interaction during irradiation is indicated to occur at the bulk nitrogen sites. Secondary Ion Mass (SIMS) depth profiles have demonstrated that the nitrogen concentration after TEM sample preparation is uniformly distributed at a level of $\sim 10^{16} \mathrm{cm}^{-3}$ [16]. Concerning the arguments about thickness differences, the topography of the irradiated surface was profiled using atomic force microscopy, but no surface topography was observed on either the top or the bottom of the TEM samples. As for the question of oxygen precipitation, it cannot be ruled out that the surface oxide has some response to irradiation. In fact, irradiation under a tightly converged beam often causes oblation of the surface oxide. In Fig. 4d, however, the energy-loss spectrum of Fig. 4e tells us that interstitial oxygen is piled up here, and this interstitial oxygen would have had to move by bulk diffusion. A similar situation is found in Fig. 6, where stacking faults have nucleated near a hole that was created during irradiation by a 2–3 nm converged electron beam. Holes like this are readily observed as a result of converged-beam irradiation in silicon thin foils, and it is often assumed to be an artifact related to surface diffusion. In this case, however, it is not possible for the stacking fault to have been nucleated by atoms diffusing along the surface because there is no driving force outside of the beam to force surface atoms into the bulk. Instead, atoms kicked out of their lattice sites have diffused in the bulk via interstitial pathways, and aligned themselves so as to lower the local energy. While some surface diffusion cannot be ruled out, it is likely that the two mechanisms compete during irradiation. In the case of Fig. 6b, however, there is no way for amorphization of the sample to occur through surface rearrangement. This result can only be explained by a bulk interaction at a high rate of damage accumulation. In N-free Si, amorphization was never achieved with a 200 kV beam, even at 15 K and with electron doses of 10^{23} cm^{-2}. In nitrogen-doped silicon, however, the nitrogen interaction is strong enough to facilitate breakdown of the crystal structure through repeated interaction with the silicon point defects.

5.2. Damage dynamics

It was noted earlier that the hole creation process in Fig. 6 does not involve nitrogen in the creation of vacancies that eventually grow to be a hole. It was determined that, based on Rutherford scattering, a 200 kV electron can impart up to 18 eV of energy to a silicon atom, see above. First principles calculations indicate that the knock-on energy to create a stable V-I pair in silicon ranges from 11–20 eV, but that Frenkel pairs created at the lower end of this energy range tend to quickly recombine in molecular dynamics simulations of the final configuration at room temperature. It is likely that this knock-on/recombination process occurs regularly during routine TEM analysis. Consider that, under typical conditions of the Topcon 002B TEM beam exposure (i.e. 10 μA, 400 nm beam diameter), $\sim 3.1 \times 10^5$ electrons will flow through an area of 0.0625 nm^2 every second [19]. Based on the graph presented in Fig. 3, the probability for each individual electron to impart more than 15 eV to one silicon atom is $P \approx 0.0000025$ [20]. Calculating the probability for interaction in one second as one minus the probability that none of the electrons will interact,

$$P(1s) = 1 - (1 - P(1e^-))^{310{,}000}$$
$$= 1 - 0.9999975^{310{,}000} \approx 0.54$$

the result is close to a coin toss. Using the same expression, the probability of an electron imparting the maximum possible energy (18.6 eV) to one of the atoms in a 100 nm thick column in 1s is 0.79! Our conjecture is that permanent separation requires a second electron collision to occur before the Frenkel pair recombines (in the absence of nitrogen). According to simulations, recombination of the V-I pair within 100 ps is quite likely [11]. However, in either the Topcon 002B or the JEOL 2010F microscope with a beam diameter of 100–400 nm, the probability of *any* electron passing by a particular place in a period of 100 ps is 3.1×10^5 e$^-$/s $\times$ 10^{-12} s $\approx$ 0.00001, and much less that an electron that will impart significant energy to the displaced atom. Under these broad-beam irradiation conditions, recombination should dominate. Hole creation is usually observed at a beam diameter of <5 nm, where the picture changes dramatically. In the JEOL 2010F, with 1 μA of beam current flowing through an area $\sim$2 nm in diameter, there will be $\sim$12 electrons passing through each 0.0625 nm^2 every 100 ps, so that a second low energy collision to further separate the Frenkel pair before recombination becomes a real possibility. The repetition of this process over several tens of seconds results in the observed rapid out-diffusion of silicon atoms from the irradiated volume via bulk and surface diffusion.

The results of the nudged elastic band calculation add an interesting follow-on to the discussion of knock-on processes. It appears that the N_2 defect causes the barrier to Frenkel pair creation to be lowered from the reported range, 11–20 eV, to a value around 6 eV. For argument, we assume a moderate value for the displacement energy: $E_d = 15$ eV. In Fig. 3, the nitrogen-enabled knock-on energy has a higher probability, $P = 0.00015$, than the 15 eV event with $P = 0.00001$ by a factor of 15. In the course of 1s irradiation, the probability of a nitrogen-enabled V-I separation at any particular N_2 site is near unity, but the probability of an event in pure silicon is still 0.54 for every atom, and there are $\sim 10^6$ as many bulk silicon atoms as there are silicon atoms near an N_2 pair, so the pure silicon interaction should still be more prevalent. Therefore the calculated lowering of the energy barrier to Frenkel pair formation is not sufficient to account for the dramatic difference in response to irradiation between nitrogen-doped and nitrogen-free samples. Two alternative arguments can be made. First, one could argue that the effective value of E_d, accounting for a temperature dependence of the spontaneous recombination volume, is actually above 18.6 eV at room temperature. This properly explains the damage observed at 15 K under electron irradiation, but is not entirely satisfying since the process of hole formation as explained above makes it clear that even the fastest recombination events can be disrupted given the right conditions. Instead, to properly account for the observed differences, the stability of the damage configuration must be examined.

The N_2V-I configuration of Fig. 7k has been shown to have an energy barrier of 1 eV against reversion to the ground state, which is well above the thermal budget (<0.1 eV) available during irradiation. Since the pure V-I pair apparently recombines spontaneously during RT irradiation, it is reasonable to conclude that its energy barrier to recombination is on the order of the thermal energy, $\sim$0.03 eV. Therefore the nitrogen-related Frenkel pair is considerably more stable than the pure Frenkel pair, allowing time for a subsequent electron collision to further evolve the system. Concerning this second event, the energy barrier to move an interstitial from the configuration of Fig. 7k to the next-nearest interstitial site is also 1 eV. This is still higher than the thermal budget (and the value for interstitial migration), and so a second electron collision is needed. Even though the energy barrier to forward diffusion is almost identical to that for reversion, the probability for a beam electron to stimulate forward momentum (consistent with direction of momentum of the e-beam) is orders of magnitude greater than that to cause backwards momentum. Ultimately, the moderate stability of the new defect is the key ingredient that enables self-interstitial migration away from its vacancy and the resulting damage accumulation that is observed in Figs 1, 4 and 5.

This theoretically determined energy barrier can now be used to estimate the probability and prevalence of the proposed N_2-assisted kick-out mechanism under real irradiation conditions. Using the value quoted above, $\sim 3.1 \times 10^5$ electrons pass through a $^1/_4$ unit cell area every second during typical irradiation. From Fig. 3, each electron has a probability of 0.00015 to transfer more than 6.2 eV to a silicon atom in a 1 nm thickness, so that each atom has a $P = 0.0000375$ chance of interacting with each electron passing within a 0.1 nm radius. Within one second, 3.1×10^5 electrons will pass within this cross-section, so the probability for interaction per second is

$$P(1s) = 1 - 0.9999625^{310,000} \approx 0.99999134$$

The relative concentration of nitrogen in the silicon is 2×10^{-7}, and each nitrogen atom in the N_2 pair has two nearest neighbors, each of which is quite likely to receive enough energy to be displaced. Presumably, some recombination will occur as a result of subsequent electron collisions because the energy barrier to reversion is only 1 eV, but the Frenkel pair is expected to be fairly stable against recombination when nitrogen is involved. The amount of damage is still likely to oscillate since the free interstitials may recombine with other vacancies as they diffuse. As interstitials occasionally and randomly leave the beam volume, however, vacancy defects will start to dominate under the beam while interstitial complexes can form just outside. In a cylindrical volume of 400 nm diameter and 100 nm thickness, there will be $\sim$60 N_2 pairs in ion milled, as-grown material, so the extent of the observed damage is reasonable, even if each N_2 pair is responsible for nucleating only one damage center.

Returning to the observation of a lateral segregation of interstitials and vacancies, see Figs 1 and 5b, the net *direction* of mass transfer during irradiation deserves some discussion. Given the directionality of the

electron beam and the related electron collisions, one might expect a net downward motion of silicon interstitials and a net upward motion of vacancies. The *lateral* distribution of silicon interstitials might then seem surprising. Consider that the component of momentum in the forward direction increases super-linearly as the impact parameter decreases (i.e. as more energy is transferred to the target atom). The initial knock-on event will necessarily result in the ejection of a silicon interstitial in the direction of the e-beam. By contrast, subsequent electron collisions on the interstitial atom are quite able to cause lateral diffusion for two reasons: (1) that a much lower energy transfer is required to move the interstitial, so a greater lateral component to the momentum transfer is likely, and (2) that once the interstitial diffuses by one step, its direction of motion becomes fairly random, especially in a disturbed lattice. For these reasons, the lateral diffusion of the silicon interstitials is quite possible and will be considerably more likely than for vacancies. In addition, as was mentioned earlier, the diffusion of interstitials out of the beam area is made more likely both by the complexing action of the nitrogen pairs and by the ability of an interstitial to diffuse multiple steps per electron collision.

Using these insights into the irradiation process, the geography of Fig. 4 can be explained from the point of view of diffusion and coarsening, as schematically illustrated in Fig. 9. First, the irradiation consists of fairly random electron stimulated diffusion events within a finite beam area, as shown in Fig. 9a. Therefore, a flux of silicon and oxygen atoms will leave the beam area near the periphery, while oxygen in the middle will tend to aggregate at nitrogen related complexes in the center and at favorable sites, such as the amorphous edge of the sample, as illustrated in Fig. 9b. The final picture, see Fig. 9c, has the central clusters consolidated and coarsened and a distinct ring of clusters around the edge of the beam. This matches the observations of Figs 4a and b, which focus on an area that was irradiated for 30 minutes. One might expect that further irradiation would eventually cause the oxygen rich particle to organize into stoichiometric silicon, which is apparently metastable under the beam.

Comparing the float zone and Czochralski samples, the dynamics of the competition of oxide precipitation with void formation should be controlled by the concentration of vacancies created relative to the oxygen concentration and by the nature of the irradiation. A schematic model of the nitrogen-enabled void/precipitate formation cycle is illustrated in Fig. 10. In the initial stages, N_2 captures a nearby vacancy directly after the collision between an electron and a silicon lattice atom. The silicon atom is now on an interstitial position and cannot recombine with its lattice site. Subsequent electron collisions can provide enough impulse to cause the silicon to diffuse interstitially. The N_2V complex can now undergo the same process to become N_2V_2. From this point, it has been shown in simulations [4] that further vacancies can accumulate, or that N_2V_2 can stably accumulate oxygen, forming N-O-V complexes that are believed to act as oxygen precipitate

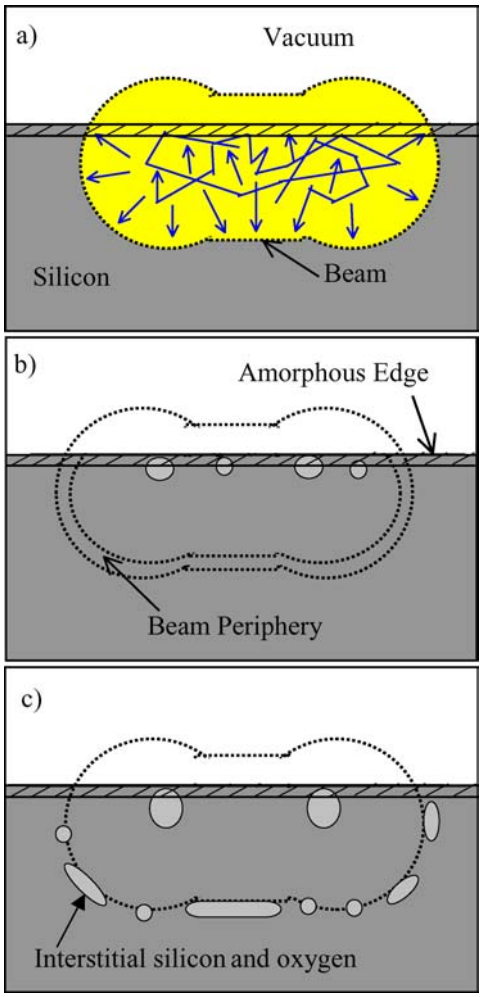

Figure 9 Illustration of a model for (a) diffusion, (b) nucleation and (c) coarsening effects observed in Fig. 4 during electron irradiation.

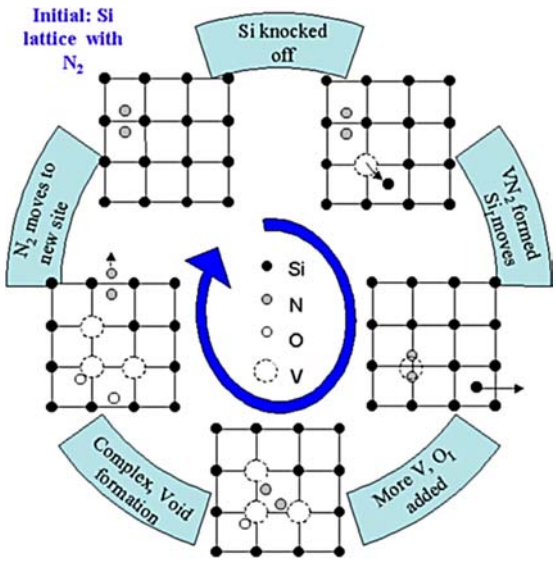

Figure 10 Model for the evolution of voids and oxygen aggregates as a result of nitrogen-assisted Frenkel pair creation during electron irradiation. The N_2 pair first facilitates V-I separation, then repeats the process to form V_2N_2, V_2N_2O, V_3N_2 and so on until the complex becomes large enough that the nitrogen diffuses away to nucleate another Frenkel pair.

nuclei. Over time, each N_2 pair could nucleate multiple extended defects by being electron stimulated to leave the now large defect that has been created, as in the last step of the cycle. The N-FZ Si sample has been shown

to follow the vacancy accumulation route, see Fig. 5, while the N-CZ Si sample clearly has oxygen precipitation as the dominant phenomenon, although small voids may also form.

6. Conclusion

The above results provide significant evidence that bulk processes dominate during 200 kV irradiation of N-CZ and N-FZ Si. Firstly, all of these phenomena are unique to silicon with bulk nitrogen doping. Since the effects are absent in otherwise identical nitrogen-free silicon, the chief irradiation process must occur in the bulk at nitrogen sites. It is possible that the dark spots in Fig. 5c are due to vacancies that aggregate at the surface to form faceted pits along {111} planes, but they were not observed by AFM. Some combination of the bulk and surface processes is perhaps the most likely. It has already been indicated that the channeling seen in Fig. 5b and the formation of a stacking fault and amorphized silicon in Fig. 6 strongly demonstrate the interstitial diffusion of silicon atoms.

There are two aspects that set this experiment apart from the wealth of irradiation studies at high voltage (300 kV and greater). First, a unique aspect of using 200 keV TEMs is that the electrons are limited by momentum conservation to transferring at most 18.7 eV of energy to a silicon atom, providing just enough impulse to create knock-ons, and not so much that cascades of damage occur. Second, using converged beams of 50–400 nm diameter allows the separation of vacancy aggregates, which form under the beam and remain there, from interstitial aggregates that are actively expelled from the beam area by electron collisions. Thus the two types of defects can be studied separately. These advantages have been used here to induce the nucleation, precipitation and coarsening of oxygen aggregates as verified by EELS, and the growth of voids by one-at-a-time addition of vacancies. Amorphization of silicon has also been induced for the first time by 200 kV irradiation, and the observation of stacking fault nucleation resulting from e-beam induced hole formation reveals the bulk nature of that interaction. Atomic-scale and nanoscale models have been presented to explain the interaction of nitrogen in the observed phenomena, from Frenkel pair formation through the formation of complexes and extended defects.

Practically, there are many possibilities for studying nanoscale material properties using the room temperature electron irradiation technique demonstrated here. The formation of voids, oxygen precipitates, and stacking faults have all been induced by exposure to the electron beam. This method can be the basis for the manipulation of crystalline/amorphous layers and the nucleation of slip dislocations, as will be shown elsewhere. This represents a laundry list of point, line and plane defects that can be studied from the earliest stages of formation, at room temperature and *in situ* in the TEM.

Most importantly, however, the fundamental nature of the interaction between 200 kV electrons and silicon atoms has been elucidated. Based on low temperature irradiation [12] and extreme current irradiation observations, it is clear that Frenkel pairs are created in the bulk by collisions with 200 kV electrons, putting the displacement energy somewhere below 18.7 eV. Very high beam currents focused on a small area have been shown to cause the formation of holes in thin films because of secondary electron collisions that can occur during the few picoseconds before recombination. At low temperature ($\sim$15 K), the thermal energy is not sufficient to surmount even the small barrier to recombination, and the defects are frozen in. While the common assumption has been that normal, RT broad beam exposure of silicon causes no damage, we propose that knock-on/recombination processes occur very frequently, causing frequent atom swaps with no *net* damage. Small amounts of nitrogen (ppm range) have been shown to enable the creation of Frenkel pairs during the irradiation of silicon. While there is a lowering of the energy barrier to Frenkel pair creation, the crucial factor in maintaining the Frenkel pair is the barrier to recombination caused by the bonding between N_2 and the vacancy. Presumably, other impurities could have the same effect, but many notable impurities apparently do not, including oxygen, phosphorus and arsenic, indicating the uniqueness of the N_2 defect in silicon.

Acknowledgements

This work is supported by NREL contract grant: AAT-2-31605-05 and by the Silicon Wafer Engineering and Defect Science I/U CRC program under NSF grant: EEC-9726176.

References

1. G. A. ROZGONYI, in "Semiconductor Silicon 2002," in Proceedings of the Electrochemical Society 2002–1 (The Electrochemical Society, New Jersey, 2002) p. 149.
2. M. TAMATSUKA, N. KOBAYASHI, S. TOBE and T. MATSUI, in Proceedings of the Electrochemical Society **99–1** (The Electrochemical Society, New Jersey, 1999) p. 456.
3. K. NAKAI, Y. INOUE, H. YOKOTA, A. IKARI, J. TAKAHASHI, A. TACHIKAWA, K. KITAHARA, Y. OHTA and W. OHASHI, *J. Appl. Phys.* **89** (2001) 4301.
4. A. KAROUI, F. S. KAROUI, G. A. ROZGONYI, M. HOURAI and K. SUEOKA, *J. Electrochem. Soc.* **150** (2003) G771.
5. H. KAGESHIMA, A. TAGUCHI and K. WADA, *Appl. Phys. Lett.* **76** (2000) 3718.
6. N. STODDARD, A. KAROUI, G. DUSCHER, A. KVIT and G. ROZGONYI, *Electrochem. Sol. State Lett.* **6** (2003) G134.
7. S. J. PENNYCOOK and L. A. BOATNER, *Nature* **366** (1988) 565.
8. P. E. BLOCHL, E. SMARGIASSI, R. CAR, D. B. LAKS, W. ANDREONI and S. T. PANTELIDES, *Phys. Rev. Lett.* **70** (1993) 2435.
9. G. D. WATKINS, *Mat. Sci. Semicond. Proc.* **3** (2000) 227.
10. R. S. AVERBACK and T. DIAZ DE LA RUBIA, *Sol. State Phys.* **51** (1997) 281.
11. W. WINDL, T. J. LENOSKY, J. D. KRESS and A. F. VOTER, *Nucl. Inst. Meth. Phys. B* **141** (1998) 61.
12. J. YAMASAKI, S. TAKEDA and K. TSUDA, *Phys. Rev. B* **65** (2002) 115213.
13. D. N. SEIDMAN, R. S. AVERBACK, P. R. OKAMOTO and A. C. BAILY, *Phys. Rev. Lett.* **58** (1987) 900.
14. L. REIMER, in "Transmission Electron Microscopy: The Physics of Image Formation and Microanalysis" (Springer-Verlag, Berlin, 1993) p. 210.

15. R. F. EGERTON, in "Electron Energy-Loss Spectroscopy in the Electron Microscope," 2nd ed. (Plenum Press, New York, 1996) pp. 137, 186.
16. N. STODDARD, G. DUSCHER, A. KAROUI, F. STEVIE and G. ROZGONYI, "Segregation and Enhanced Diffusion of Nitrogen in Silicon Induced by Low Energy Ion Bombardment," Submitted to J. Appl. Phys, 2004.
17. H. SAWADA, K. KAWAKAMI, A. IKARI and W. OHASHI, *Phys. Rev. B* **65** (2002) 075201.
18. V. S. VAVILOV, A. E. KIV and O. R. NIYAZOVA, *Phys. Stat. Sol.* **(a)32** (1975) 11.
19. This area is 1/4 the area of one side of the Si unit cell, about the interaction area of a beam electron
20. This is the probability for interaction in 1 nm thickness, 0.00001, divided by the 4 atoms in 1/4 of the unit cell area over two unit cells' thickness

Received 25 October 2004
and accepted 2 March 2005